

## 3D stability analysis of convex slopes in plan view using lower bound linear finite element

F. Askari<sup>1,\*</sup>, A. Totonchi<sup>2</sup>, O. Farzaneh<sup>3</sup>

Received: December 2011, Accepted: August 2011

### Abstract

*Presented is a method of three-dimensional stability analysis of convex slopes in plan view based on the Lower-bound theorem of the limit analysis approach. The method's aim is to determine the factor of safety of such slopes using numerical linear finite element and lower bound limit analysis method to produce some stability charts for three dimensional (3D) homogeneous convex slopes. Although the conventional two and three dimension limit equilibrium method (LEM) is used more often in practice for evaluating slope stability, the accuracy of the method is often questioned due to the underlying assumptions that it makes. The rigorous limit analysis results in this paper together with results of other researchers were found to bracket the slope stability number to within  $\pm 10\%$  or better and therefore can be used to benchmark for solutions from other methods. It was found that using a two dimensional (2D) analysis to analyze a 3D problem will leads to a significant difference in the factors of safety depending on the slope geometries. Numerical 3D results of proposed algorithm are presented in the form of some dimensionless graphs which can be a convenient tool to be used by practicing engineers to estimate the initial stability for excavated or man-made slopes.*

*Keywords: three-dimensional slope, slope stability, limit analysis, Lower-bound, limit equilibrium*

### 1. Introduction

The assessment of slope stability has received much attention across geotechnical communities because of its practical importance. This problem has drawn the attention of many investigators [1–7] in the past and continues to do so. Limit-equilibrium analysis has been the most popular method for slope stability calculations. A major advantage of this approach is that complex soil profiles, seepage, and a variety of loading conditions can be easily dealt with. Two dimensional (2D) limit equilibrium analyses, such as Bishop's simplified method [2] and Janbu's simplified method [7], are two of the most popular approaches used to evaluate slope stability. It is commonly believed that 2D solutions utilized in design will obtain a conservative evaluation for a three dimensional (3D) slope failure. However, as pointed out by Gens et al. [8], estimates of the mobilized shear strength

derived from the 2D back analysis for a 3D slope, will be unsafe.

In order to account for the three dimensional effects on slope stability many 3D methods had been proposed [9–11]. The majority of methods proposed in these studies are simply based on extensions of Bishop's simplified [2], Spencer's [12], or Morgenstern and Price's [13] original 2D limit equilibrium slice methods. Many comparisons of limit-equilibrium methods indicate that techniques that satisfy all conditions of global equilibrium give similar results. Regardless of the different assumptions about the interslice forces, these methods give values of the safety factor that differ by no more than 5%. Even though it does not satisfy all conditions of global equilibrium, Bishop's simplified method also gives very similar results. Partly because of this and partly because of its simplicity, the slice method of limit-equilibrium analysis proposed by Bishop [2] has been used widely for predicting slope stability. Because of the approximate and somewhat arbitrary nature of limit-equilibrium analysis, concern is often voiced about how accurate these types of solutions really are. Using the limit theorems can not only provide a simple and useful way of analyzing the stability of geotechnical structures, but also avoid the shortcomings of the arbitrary assumptions underpinning the LEM.

\* Corresponding Author: Askari@iiees.ac.ir

<sup>1</sup> Assistant Professor, Iran International Earthquake Engineering Institute, Tehran, I. R. of Iran

<sup>2</sup> Assistant Professor, Department of Civil Engineering, Marvdasht Branch, Islamic Azad University, Marvdasht, I. R. of Iran

<sup>3</sup> Assistant Professor, Department. of civil Engineering, Tehran University, Tehran, I. R. of Iran

Numerous methods have been proposed for slope stability analysis. In general, these methods can be classified into the following types: (1) limit equilibrium approach which is the most common; (2) numerical solutions based on Finite Element Method; and (3) limit analysis approach.

Stability problems of slopes are often analyzed by methods based on two-dimensional models, neglecting the end effects of the failure mechanism. However, the failure regions of actual slopes usually have finite dimensions and therefore a three-dimensional (3D) approach is more appropriate to analyze such stability problems. 3D slope stability problems fall into three categories:

1. Slopes that are subjected to loads of limited extent at the top.
2. Slopes in which the potential failure surface is constrained by physical boundaries, such as a dam in a narrow rock-walled valley.
3. Slopes with nonplanar surfaces such as road embankments at curves, or mining waste where the granular material heaps have well-defined corners.

Most analyses for slope stability have dealt with straight slopes with a planar surface. However, there are many convex slopes in plan view with nonplanar surfaces. During the past decades, the influence of plan curvature on the stability of slopes has been investigated mainly by Leshchinsky and Baker [11], Giger and Krizek [14,15], Baker and Leshchinsky [16], Xing [17], and Ohlmacher [18] for some special cases. Giger and Krizek [14,15] used the upper-bound theorem of limit analysis to study the stability of a vertical corner cut subjected to a local load. They assumed a kinematically admissible collapse mechanism and, through a formal energy formulation, assessed the stability with respect to shear strength of soil. Leshchinsky et al. [19] presented a 3D analysis of slope stability based on the variational limiting equilibrium approach and proved that it can be considered as a rigorous upper bound in limit analysis. Leshchinsky and Baker [11] used a modified solution of the approach mentioned to study 3D end effects on stability of homogeneous slopes constrained in the third direction and applied it to investigate the stability of vertical corner cuts. Using a variational approach, Baker and Leshchinsky [16] discussed the stability of conical heaps formed by homogeneous soils. Xing [17] proposed a 3D stability analysis for concave slopes in plan view using the equilibrium concept. Based on the limit equilibrium method, Ohlmacher [18] investigated a case study including convex and concave slopes.

Michalowski [20] introduced a rigorous 3D approach in the strict framework of limit analysis for homogeneous and straight slopes. In his analysis, the geometry of slope and slip surface was unrestricted and both cohesive and frictional soils were included. Farzaneh and Askari [21] improved Michalowski's algorithm in the case of 3D homogeneous slopes and extended it to analyze the stability of nonhomogeneous slopes. Duncan [22] provides a comprehensive review for two dimensional (2D) and three dimensional (3D) LEM and FEM estimates of slope stability, and therefore the review of literature herein will be referring to more recent publications (post 1996).

In most cases it is not feasible to perform a full displacement finite element analysis and as such the three dimensional

effects of the slope in question are often ignored. However, ignoring the 3D effects when analyzing slopes can lead to unsafe answers. In the back analyses of shear strengths, for example, neglecting the 3D effects will lead to values that are too high, and therefore affect any further stability assessments at the same location. As stated previously, one aim of this study is to produce 3D stability charts that can be used by practicing engineers, extending those currently used regularly for 2D slope stability evaluation.

This paper is devoted to use linear finite element, lower-bound solution method and an optimization approach to make the maximum lower bound solutions for 3D convex slope stability. The main purpose of this paper is to provide sets of 3D stability charts for homogeneous soil slopes by using the finite element lower bounding method and upper-bound results of Farzaneh and Askari [23] which can bracket the actual stability numbers from above and below. The chart solutions in this study can be seen as convenient tools to be used by practicing engineers to estimate the initial stability for excavated or man-made slopes.

## 2. Background

Figure 1 shows a typical load-displacement curve as it might be measured for a surface footing test. The curve consists of an elastic portion; a region of transition from mainly elastic to mainly plastic behavior; a plastic region, in which the load increases very little while the deflection increases manifold; and finally, a work-hardening region. In a case such as this, there exists no physical collapse load. However, to know the load at which the footing will deform excessively has obvious practical importance. For this purpose, idealizing the soil as a perfectly plastic medium and neglecting the changes in geometry lead to the condition in which displacements can increase without limit while the load is held constant as shown in Fig. 1. A load computed on the basis of this ideal situation is called plastic limit load [21]. This hypothetical limit load usually gives a good approximation to the physical plastic collapse load or the load at which deformations become excessive. The methods of limit analysis furnish bounding estimates to this hypothetical limit load.

The theorems of limit analysis can be established directly for a general body if the body possesses the following ideal properties:

1. The material exhibits perfect or ideal plasticity, i.e., work hardening or work softening does not occur. This implies that stress point can not move outside the yield surface.
2. The yield surface is convex and the plastic strain rates are

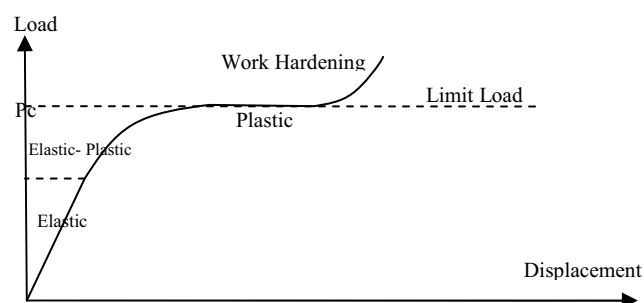


Fig. 1. Load-displacement curve

derivable from the yield function through the associated flow rule.

3. Changes in geometry of the body that occur at the limit load are in significant; hence the equations of virtual work can be applied.

The limit analysis method models of the soil as a perfectly plastic material obeying an associated flow rule. With this idealization of the soil behavior, two plastic bounding theorems (lower and upper bounds) can be proved. According to the upper bound theorem, if a set of external loads acts on a failure mechanism and the work done by the external loads in an increment of displacement equals the work done by the internal stresses, the external loads obtained are not lower than the true collapse loads. It is noted that the external loads are not necessarily in equilibrium with the internal stresses and the mechanism of failure is not necessarily the actual failure mechanism. By examining different mechanisms, the best (least) upper bound value may be found. The lower bound theorem states if an equilibrium distribution of stress covering the whole body can be found that balances a set of external loads on the stress boundary and is nowhere above the failure criterion of the material, the external loads are not higher than the true collapse loads. It is noted that in the lower bound theorem, the strain and displacements are not considered and that the state of stress is not necessarily the actual state of stress at collapse. By examining different admissible states of stress, the best (highest) lower bound value may be found.

The bound theorems of limit analysis are particularly useful if both upper and lower bound solutions can be calculated, because the true collapse load can then be bracketed from above and below. This feature is invaluable in cases for which an exact solution cannot be determined (such as slope stability problems), because it provides a built-in error check on the accuracy of the approximate collapse load.

Although the limit theorems provide a simple and useful way of analyzing the stability of geotechnical structures, they have not been widely applied to the 3D slope stability problem. Currently, most slope stability evaluations based on the limit theorems have used the upper bound method alone, such as Chen et al. [24,25], Donald and Chen [26], Farzaneh and Askari [21], De Buhan and Garnier [27], Michalowski [5,28-29], and Viratjandr and Michalowski [30]. Major contributions for soil slope stability analysis were presented by Michalowski and his co-worker who investigated local footing load effects on the 3D slope stability [5] and provided sets of stability charts for cohesive-frictional slopes which took seismic loadings and pore pressure into account. In addition, Michalowski [29] employed the limit analysis technique to estimate the stability of uniformly reinforced slopes.

Because of the difficulties of constructing statically admissible stress fields manually, the application of limit analysis has in the past almost exclusively concentrated on the upper bound method. In fact, the authors are not aware of any rigorous lower bound solutions for the stability of slopes in cohesive-frictional soils. Although the upper bound solutions may be used as an estimate for the true collapse load, it is the lower bound solutions that are generally more useful in practice, because they are inherently conservative.

A lower bound solution is obtained by insisting that the stresses obey equilibrium and satisfy both the stress boundary

conditions and the yield criterion. Each of these requirements imposes a separate set of constraints on the nodal stresses. In the lower bound finite-element analysis, statically admissible stress discontinuities are permitted at edges shared by adjacent triangles and also along borders between adjacent rectangular extension elements. The finite element lower bound limit analysis techniques developed by Lyamin and Sloan [31] and Krabbenhoft et al. [32] provide a useful method for dealing with the problems of slope stability (Appendix 1). These numerical lower bound methods have been used to provide chart solutions by Yu et al. [33] for 2D purely cohesive and cohesive-frictional soil slopes. In this paper, similar formulations are used and described with newly types of elements for investigating the effect of convexity in slopes.

## Proposed Solution

Consider a body with a volume  $V$  and surface area  $A$ , as shown in Fig.2. Let  $t$  and  $q$  denote, respectively, a set of fixed tractions acting on the surface area  $A_t$  and a set of unknown tractions acting on the surface area  $A_q$ . Similarly, let  $g$  and  $h$  be a system of fixed and unknown body forces which act, respectively, on the volume  $V$ . Under these conditions, the objective of a lower bound calculation is to find a stress distribution which satisfies equilibrium throughout  $V$ , balances the prescribed tractions  $t$  on  $A_t$ , nowhere violates the yield criterion, and maximizes the integral

$$Q = \int_{A_q} q \, dA + \int_V h \, dV \quad (1)$$

Since this problem can be solved analytically for a few simple cases only, it is searched a discrete numerical formulation which can model the stress field for problems with complex geometries, inhomogeneous material properties, and complicated loading patterns. The most appropriate method for this task is the finite element method.

Disregarding, for the moment, the type of element that is used to approximate the stress field, any discrete formulation of the lower bound theorem leads to a constrained optimization problem of the form

$$\begin{aligned} &\text{Maximize Objective Function} && \text{subject to} \\ &a_i(x) = 0, \quad i \in I = \{1, \dots, m\} \\ &f_j(x) \leq 0, \quad j \in J = \{1, \dots, r\} \\ &x \in R^n \end{aligned} \quad (2)$$

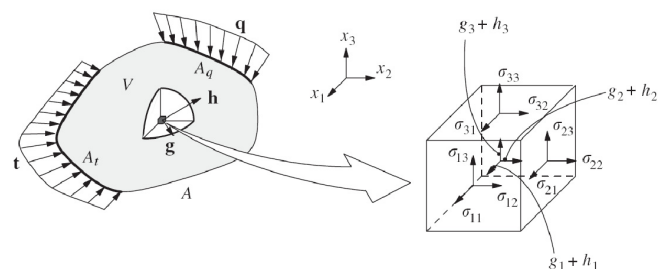


Fig. 2. A body subjected to the surfaces and body forces [31]

where  $x$  is an  $n$ -dimensional vector of stress and body force variables. The equalities defined by the functions  $a_i$  follow from the element equilibrium, discontinuity equilibrium, and boundary and loading conditions, while the inequalities defined by the functions  $f_j$  arise because of the yield constraints and the constraints on applied forces. Here Objective Function is described as safety factor of a three dimensional slopes and  $a_i$  is a global matrix which contains equilibrium, discontinuity and boundary equations. In addition,  $f_j$  produces the conditions which nodal stresses will be less than the yield surface. Maximizing Objective Function leads to use an optimization approach. In this paper the nonlinear optimization based on a fast quasi-Newton method whose iteration count is largely independent of the mesh refinement, is selected for finding the maximum lower-bound solution of safety factor which satisfying the element equilibrium, discontinuity equilibrium, and boundary and loading conditions. The global form of each element in this solution is shown in Fig. 3. As it is seen the stresses variation between each nodes of element is assumed to be linear, thus this type of finite element is called Linear Finite Element. The following section gives a detailed description of the discretization procedure for the case of 3-dimensional linear elements.

Unlike the usual form of the finite element method in which each node is unique to a particular element, multiple nodes can share the same coordinates, and statically admissible stress discontinuities are permitted at all interelement boundaries. The typical 3D slope geometry details for the problem of this paper are shown in Fig. 4.

In this paper, all models are organized from some prismatic units as is shown in Fig. 5. Using this type of unit as a base of modelings, all kind of straight, convex, concave and every

other arbitrary shape in plan view of slopes can be created. Each discussed unit is combined from three volumetric pyramid elements which are shown in Fig. 6.

The global form of modellings is consisted of two plans which one locates at the top and the other at the bottom of the model. Fig. 7. shows the top and bottom plans of modelling. Between each pair of slices in the plans (1 to 12), 3 elements in the form of a prismatic unit shown in Fig. 5 are constituted. For higher slopes, various numbers of prismatic units are used in the height of the slopes.

The typical 3D slope model for the problem of this paper is shown in Fig. 8. This model is consisted of 12 units and therefore 36 elements.

The extension elements may be used to extend the solution over a semi-infinite domain and therefore provide a complete statically admissible stress field for infinite half-space problems. In fact, the extension elements shown in Fig. 7 can be used readily to extend the stress fields into a semi-infinite domain which is discussed afterwards. Because this paper is concerned mainly with the stability of finite slopes resting on a firm base, extension elements are needed only behind of slopes (shown in Fig. 7).

### 3. Objective function and loading constraints

The purpose of lower bound limit analysis is to find a statically admissible stress field which maximizes the objective function carried by a combination of surface tractions and body forces (Figure 2). The distribution of the latter may either be known or unknown, depending on the problem. In the terminology of slopes stability, safety factor is known as the objective function, since this is the quantity it is wanted to maximize in lower bound case. Otherwise the general form of

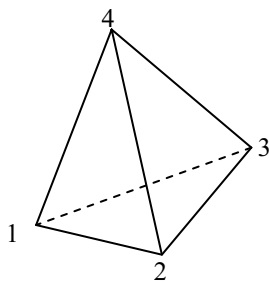


Fig. 3. Global form of elements

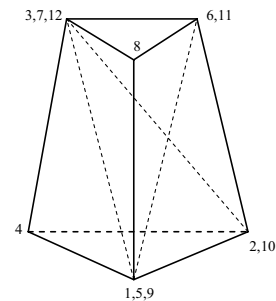


Fig. 5. Prismatic unit of modelings

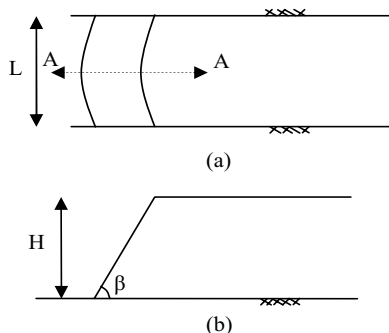


Fig. 4. Geometry details of problem (a). Plan (b). Section A-A

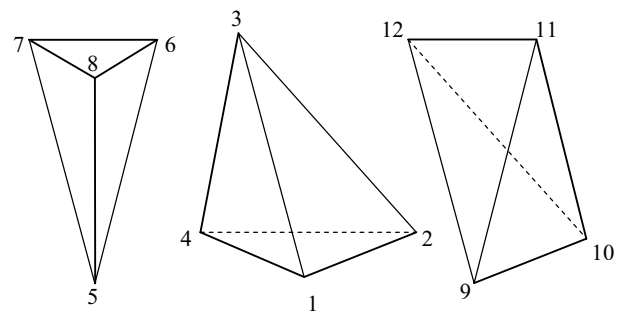


Fig. 6. Elements used for Lower Bound Limit Analysis

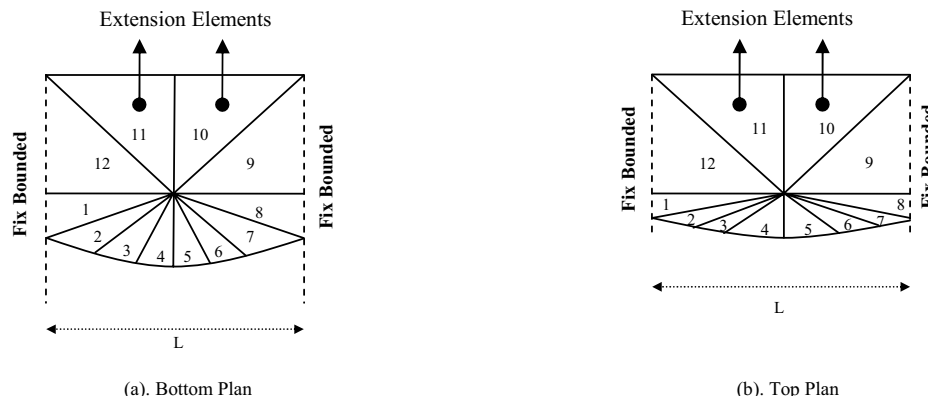


Fig. 7. Bottom and top plans of modelling, extension of the stress fields into a semi-infinite domain

the yield condition for a perfectly plastic solid has the form

$$f(\sigma_{ij}) \leq 0 \quad (3)$$

Where  $f$  is a convex function of the stress components and material constants. The solution procedure presented later in this paper does not depend on a particular type of yield function, but does require it to be convex and smooth. Convexity is necessary to ensure the solution obtained from the optimization process is the global optimum, and is actually guaranteed by the assumptions of perfect plasticity. Smoothness is essential because the solution algorithm needs to compute first and second derivatives of the yield function with respect to the unknown stresses. For yield functions which have singularities in their derivatives, such as the Mohr–Coulomb criteria, it is necessary to adopt a smooth approximation of the original yield surface. A plot of this function in the meridional plane is shown in Fig.9.

Defining tensile stresses as positive, the Mohr–Coulomb yield function may be written as

$$f = (\sigma_1 - \sigma_2) + (\sigma_1 + \sigma_2) \sin \phi_d - 2c_d \cos \phi_d \quad (4)$$

where the principal stresses are ordered so that  $\sigma_1 > \sigma_2 > \sigma_3$  and  $c_d$  and  $\phi_d$  are

$$F_{s_c} = c/c_d \quad (5)$$

$$F_{s_\phi} = \tan(\phi)/\tan(\phi_d) \quad (6)$$

which  $C$  and  $\phi$  denote, respectively, the cohesion and friction

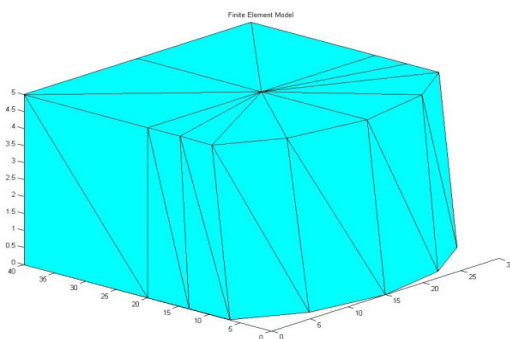


Fig. 8. Finite element Model

angle of the soil. Assuming  $F_s = F_{s_c} = F_{s_\phi}$  the objective function define as maximizing the safety factor by satisfying the yield function. This implies that the stresses at all nodes in the finite element model must satisfy the yield condition.

Thus, in total, the yield conditions give rise to some non-linear inequality constraints (considering composite yield criteria as one constraint) on the nodal stresses. Because each node is associated with a unique set of stress variables, it follows that each yield inequality is a function of an uncoupled set of stress variables  $\sigma_{ij}$ . Each admissible stress field has its own safety factor. Using an optimization method of nonlinear programming which is based on Newton's method the highest lower bound safety factor is attained. In this method, the non-linear equations at the current point  $k$  are linearized and the resulting system of linear equations is solved to obtain a new point  $k + 1$ . The process is repeated until the governing system of non-linear equations is satisfied. Thus, the highest lower bound safety factor of admissible stress fields is searched; this feature can be exploited to give a very efficient solution algorithm.

#### 4. Extension of Stress Field into Semi-infinite Domain

When the lower bound method described previously is applied to problems with semi-infinite domains, only part of the body is discretised. This means that the optimized stress field does not necessarily satisfy equilibrium, the stress boundary conditions and the yield criterion throughout the entire domain and, therefore, cannot be used to infer a rigorous lower bound on the collapse load. Although this type of solution, which is known as a partial stress field, may actually furnish a good estimate of the true collapse load, a fully rigorous lower bound can be obtained only by extending the stress field over the semi-infinite domain in such a way that all the conditions of the lower bound theorem

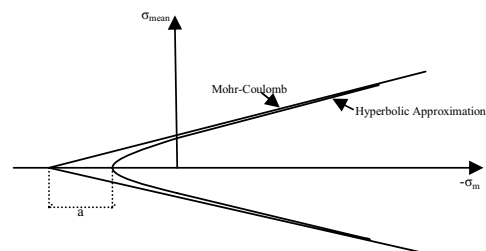


Fig. 9. Hyperbolic approximation to Mohr–Coulomb yield function

are fulfilled. This process is often difficult, especially for cases involving irregular boundary shapes, and is frequently omitted in hand calculations.

To resolve this situation some extension elements which are deployed around the periphery of the mesh are used. These are constructed so that they extend the stress field beyond the limits of the grid in such a way that it is statically admissible.

A  $D$ -dimensional extension element is much like a regular lower bound finite element in that the stress field is defined by the stresses at  $D+1$  nodes and the body forces are assumed to be constant. Indeed, as with any lower bound element, the stresses must satisfy the equilibrium, stress boundary and yield conditions. Consider the 2D case shown in Figure 10, where a linear expansion is used to model the stresses across and outside a three-noded extension element. Provided the equilibrium and stress boundary conditions are satisfied within the triangle, then they are automatically satisfied for any point  $p$  outside the triangle. This implies that all extension elements are subject to the same equilibrium and stress boundary constraints as regular elements. For  $D$ -dimensional geometries, a maximum of  $D$  different types of extension elements are required. Although they are restricted to certain types of yield criteria, extension elements are attractive because they guarantee that the solution obtained is a rigorous lower bound [31].

The proposed algorithm is concerned with the following domains:

1. Mesh generating using top and below plans
2. Deriving equilibrium, discontinuity and boundary matrices for each element
3. Deriving  $A_{\text{global}}$  in which attains following equation:

$$A_{\text{global}} x^e = b_{\text{global}} \quad (7)$$

Where  $x^e$  is unknown vector which includes the stresses in each node and the safety factor.

4. Optimizing process: This optimization is ascribing to check the maximum lower bound solution using nonlinear programming.

5. Constrains: This algorithm contains both equality and inequality constrains. The equality constrain is summarized in a global matrix contains equilibrium, discontinuity and boundary equations and the inequality constrains are refer to a. Yield Surface and b. Extension elements.

The typical lower bound finite element meshes and boundary conditions used to analyze the 3D slope problem are illustrated in Fig. 8. The stability of homogeneous slopes is usually expressed in terms of two dimensionless stability numbers in the following form

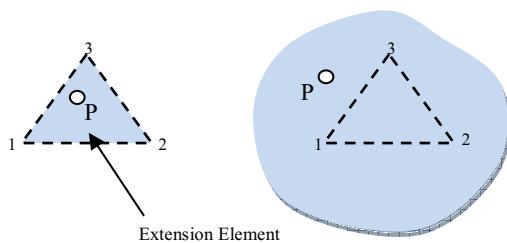


Fig. 10. Approximation of stress field inside and outside the extension element

$$N_s = \gamma H F_s / c \quad (8)$$

$$\lambda_{\phi c} = N_s \tan \phi / F_s \quad (9)$$

where  $N_s$  is the stability number,  $\gamma$  is the soil unit weight,  $H$  is the slope height,  $F_s$  is the safety factor of the slope. Also  $c$  and  $\phi$  are known as the strength parameters of the material;  $c$  represents the cohesion and  $\phi$  represents the angle of internal friction.

## 5. Comparison with other results

One of the most important parameter in analyzing is number of used elements in models. Certainly, increasing of this quantity leads to increase the accuracy of the results. But using high number of elements in modelling is caused to make time consuming runs, therefore some models were made to compare the results by different number of elements and therefore make a decision on number of elements to use and suitable time taken in each run.

For constant quantity of slope angle  $\beta=30$  and  $\lambda_{\phi c}=2$ , the results of some straight slopes for  $En=18, 24, 36$  and  $72$  are compared which is shown in Fig. 11. Where  $\beta$  is degree of the slope and  $En$  is number of used elements. As it is seen, increasing in  $En$  results in decreasing the interspaces between lower bound and upper bound solutions. It means that by increasing  $En$ , the accuracy of results is increased but its rate decreases, as Fig. 11 shows. Therefore it can be concluded that for higher number of elements, the difference between results can be connivance. Thus in this paper, all numerical results are made of 36 element because of low rate of variations afterwards (Each run approximately consumes 12 minutes). For a validation, the results of the current approach can be compared with those of other investigators for straight slopes. Fig. 12 and 13 show a sample of this modelling and the forms of the plans, respectively. Different methods have been proposed for 3D analysis of straight slopes by Baligh and

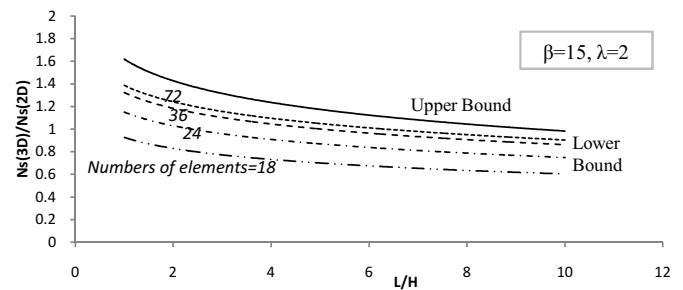


Fig. 11. Effect of element numbers in accuracy of results

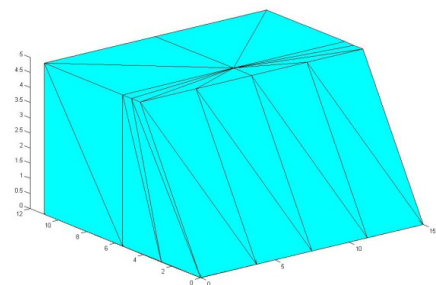


Fig. 11. Effect of element numbers in accuracy of results

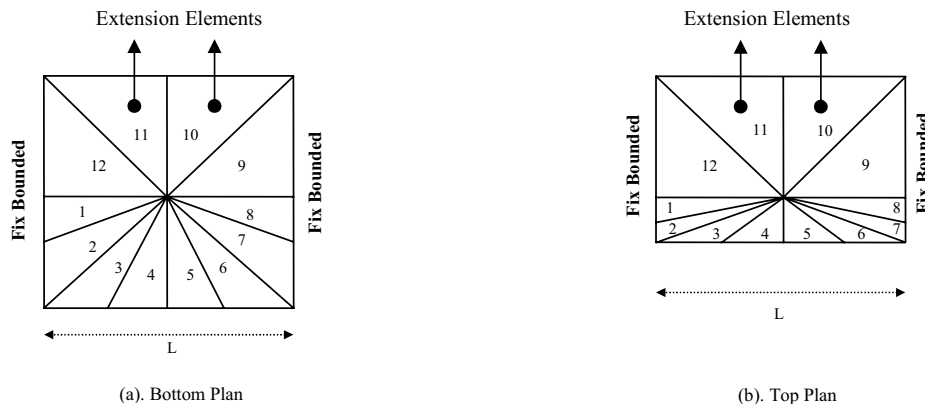


Fig. 13. Bottom and top plans of modelling for a straight slope

Azzouz [34], Hovland[9], Ugai [35], and Leshchinsky and Baker [11]. Comparing the current results with most of these, good agreement is found among them. Ugai [35] extended Baker variational limiting equilibrium approach to 3D cohesive slopes. Leshchinsky and Baker [11] extended a modified solution of variational approach in 3D stability of slopes which has been proved by them to be equivalent to the upper bound solution in the framework of limit analysis.

Fig. 14 shows the ratio  $F_{3D}/F_{2D}$  ( $F_{iD}$  is the safety factor in  $iD$  analysis) as a function of  $L/H$  obtained by Ugai [35], Leshchinsky and Baker [11], Farzaneh and Askari [36] (the upper-bound solution) and the present solution. As it is seen, the results of current solution underestimate in good accuracy.

## 6. Numerical Results

### 1.6. Stability charts for homogeneous convex slopes based on the numerical limit analyses

The 3D chart solutions for homogeneous convex slopes in plan view obtained from the numerical upper and lower bound analysis are displayed in Figs. 15-18 for a range of slope angles ( $\beta$ ), the relative curvature radius of slope ( $R_0/H$ ) and  $L/2H$  ratios. The stability numbers for 2D case are obtained from bishop's simplified method. It can be noted that the upper and lower bound limit analysis solutions bracket a range of stability numbers ( $N_s$ ) to within  $\pm 10\%$  or better for 3D cases. The upper bound results were collected from Farzaneh and Askari [36]. As it is seen no particular trend of the greatest difference in the

upper and lower bound solutions was observed.

As expected, the stability number  $N_s$  decreases when  $\beta$  and the  $L/2H$  ratio increase. For a given  $\beta$ ,  $N_s$  achieve the minimum value when  $L/2H$  goes to infinite. This implies that the factor of safety will re-duce with increasing  $L/2H$  ratio. As is known, the plain strain analysis does not consider the resistance provided by the two curved ends of the slip surface. The boundary resistance from these two curved ends can be seen as 3D end boundary effect which makes the slope more stable. While increasing the  $L/2H$  ratio, the relative contributions of resistances provided by these two curved ends decrease which means that 3D end boundary effect reduces. Therefore, using 2D stability numbers will lead to a more conservative slope design.

Fig. 15-18 presents the stability numbers ( $N_s$ ) obtained from the upper and lower bound limit analyses for various slope angles. These numbers can be used for estimating the stability of the convex slopes without retaining walls and props. A comparison of the equivalent 2D and 3D cases can be made by investigating the factor of safety ratio  $F_{3D}/F_{2D}$  for the same slope angle ( $\beta$ ), slope height ( $H$ ), unit weight ( $\gamma$ ) and dimensionless parameter ( $\lambda$ ). The ratio  $F_{3D}/F_{2D}$  is simply the ratio of the stability numbers ( $N_s$ )<sub>3D</sub>/ $(N_s)$ <sub>2D</sub>. Changing the relative curvature radius of slope ( $R_0/H$ ) shows that convex slopes in plan view are more stable than straight slopes. In general, the smaller the ratio  $R_0/H_0$  is, the higher the stability of convex slope in plan view. It should be mentioned that with decreasing  $\lambda_{\phi c}$ , three-dimensional effects are more significant. In other words, the effect of curvature of slope is more important in cohesive soils. Also it can be concluded that the effect of curvature on the stability of convex slopes is less for steeper slopes.

## 7. Example of Application

In order to make comparisons of the factor of safety between the newly proposed 3D chart solutions and the 2D solution using bishop's simplified method, an example is introduced. A U-shape slope descriptions are as follows: the slope inclination  $\beta=60^\circ$ , the height of the slope is  $H = 10$  m, width of the slope is  $L=40$  m, the soil unit weight is  $\gamma = 18.5$  kN/m<sup>3</sup>, the friction angle is  $\Phi = 10^\circ$  degree and the cohesion is  $C=32.5$  kPa.

A procedure for obtaining the factor of safety by using the

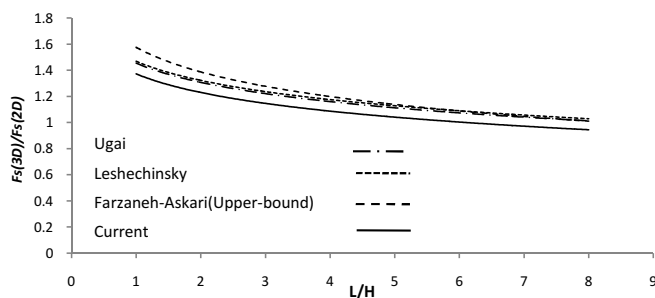


Fig. 14. Comparison with those of Ugai, Leshchinsky, Farzaneh-Askari in cohesive soil

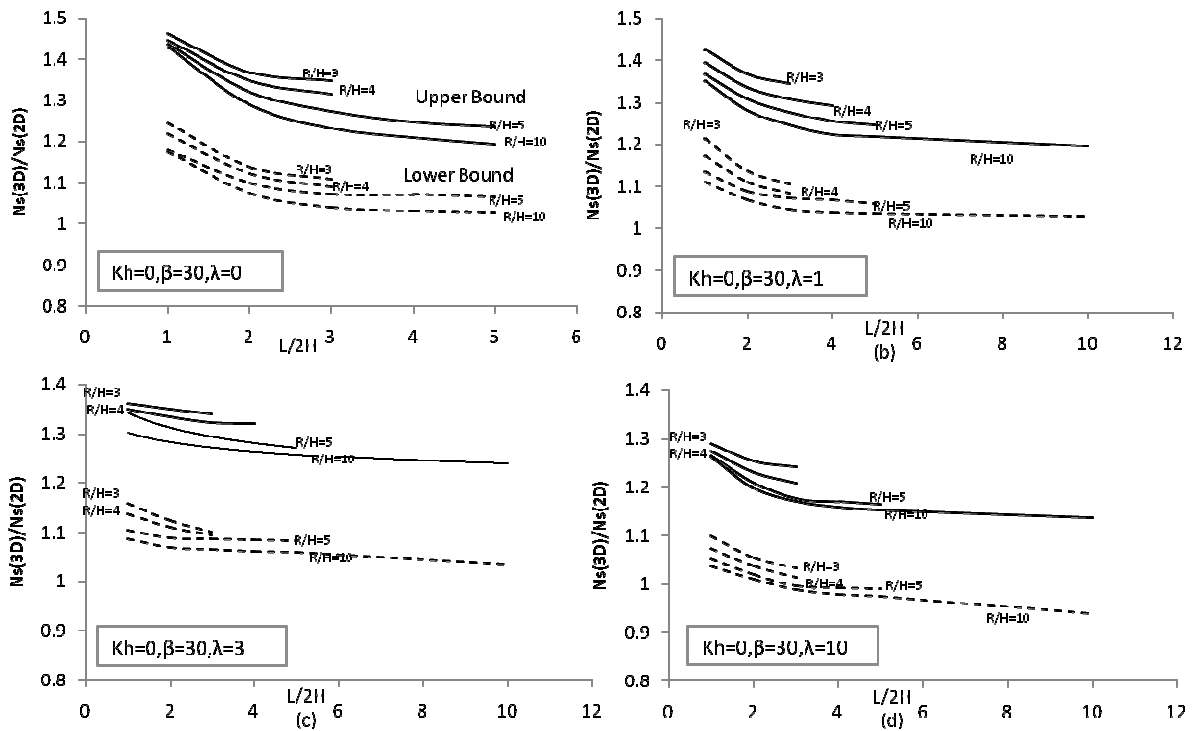


Fig. 15. Limit Analysis solution of stability numbers for  $\beta=30$  and (a).  $\lambda=0$ ; (b).  $\lambda=1$ ; (c).  $\lambda=3$ ; (d).  $\lambda=10$

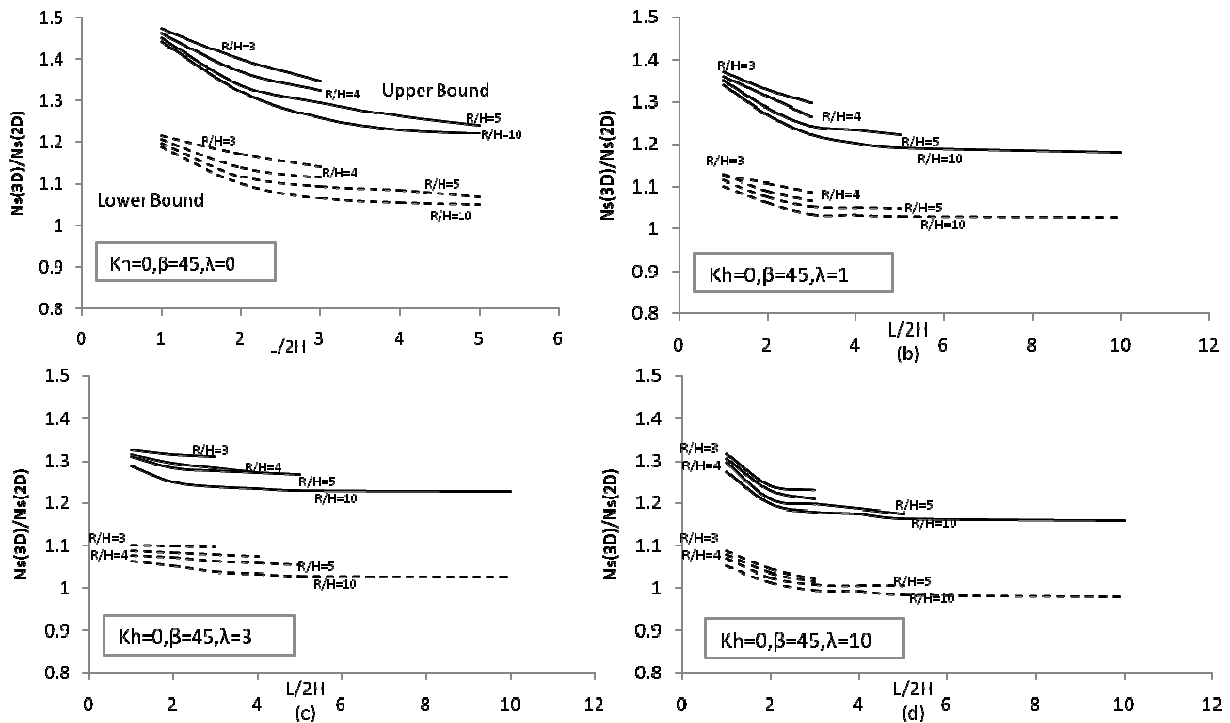


Fig. 16. Analysis solution of stability numbers for  $\beta=45$  and (a).  $\lambda=0$ ; (b).  $\lambda=1$ ; (c).  $\lambda=3$ ; (d).  $\lambda=10$

chart solutions presented in this study can be summarized in the following stages.

1. From the slope descriptions, the non-dimensional parameters  $\lambda = (18.5 \times 10 / 32.5) \times \tan 10^\circ = 1$ .
2. For  $\beta = 60^\circ$ , the chart solutions shown in Fig. 17b is employed to determine the safety factor.
3. In Fig. 17b, a straight line passing through the  $L/2H = 2$  is

plotted. This straight line intersects with the upper and lower bound curves, which are the 3D chart solutions of the numerical limit analysis.

4. The stability number from 2D limit equilibrium method is  $Ns_{(2D)} = 7.5$ . From this intersection points, it can back-figure the dimensionless parameter  $Ns_{(3D)}/Ns_{(2D)}$  from which the lower bound and the upper bound solutions become as

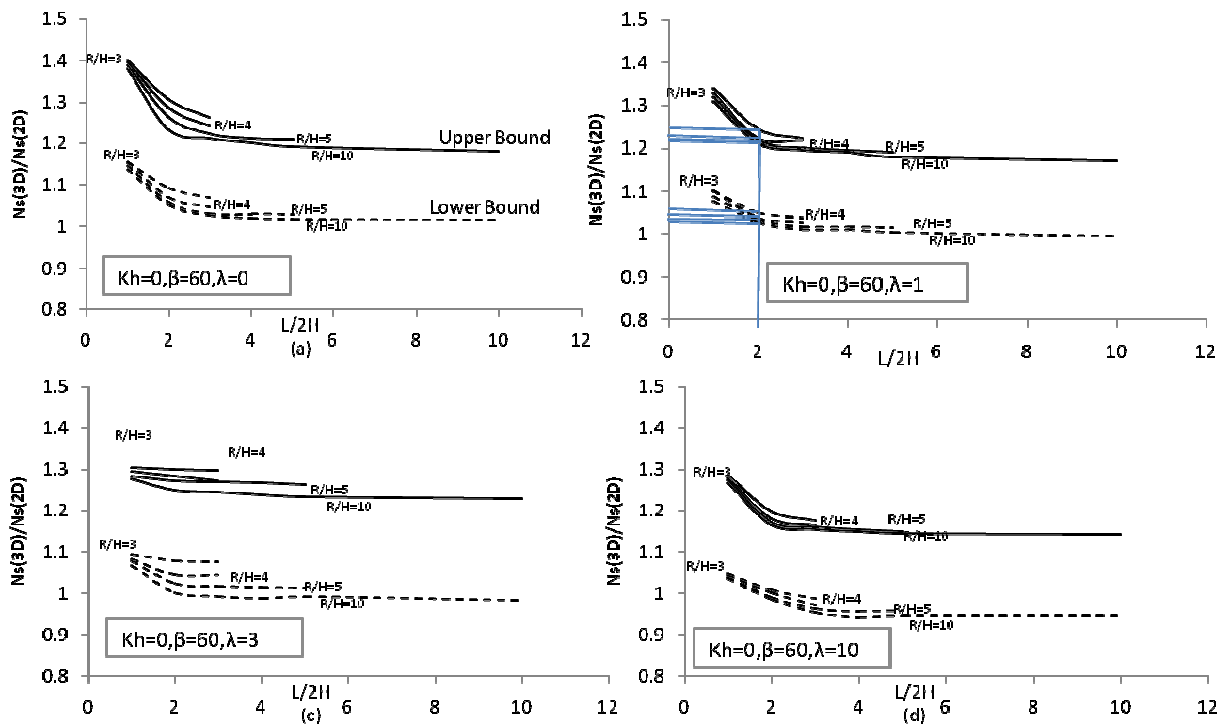


Fig. 17. Limit Analysis solution of stability numbers for  $\beta=30$  and (a).  $\lambda=0$ ; (b).  $\lambda=1$ ; (c).  $\lambda=3$ ; (d).  $\lambda=10$

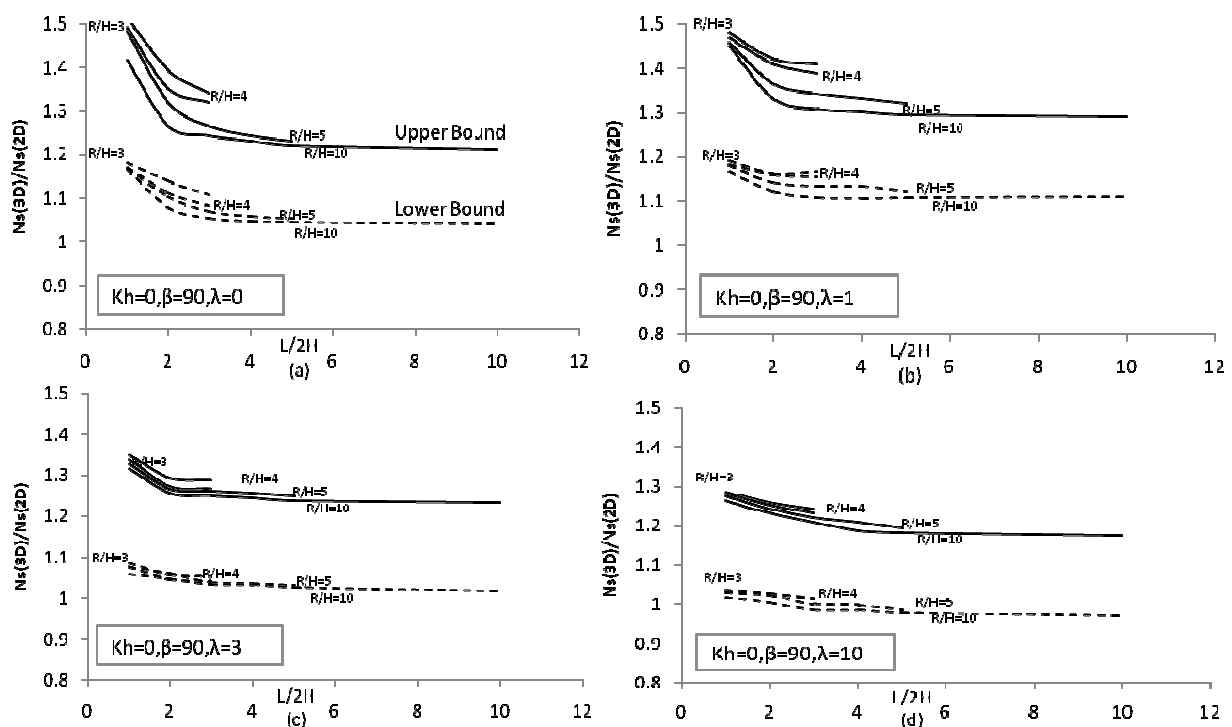


Fig. 18. Analysis solution of stability numbers for  $\beta=45$  and (a).  $\lambda=0$ ; (b).  $\lambda=1$ ; (c).  $\lambda=3$ ; (d).  $\lambda=10$

Table.1.

The averages of the upper and lower bound safety factors of  $R/H=3, 4, 5$  and  $10$  for  $L/2H=2$  are  $1.525, 1.485, 1.478$  and  $1.468$ ; respectively. The safety factors for the 3D solutions are around  $1$  to  $1.17$  times that of the safety factors of the 2D solutions. This demonstrates that the factor of safety obtained from 3D analysis will be always larger or equal to that

obtained from 2D analysis in convex slopes. Therefore, using 2D solution is conservative for design and non-conservative when determining strength parameters from a back analysis of a failed slope. In addition the difference between the upper and lower-bound factors of safety for this example is found to be around  $17\%$ . This difference decreases slightly when the ratio of  $L/2H$  increases.

## 8. Conclusions

Three dimensional stability charts for homogeneous cohesive slopes have been proposed in this paper. Based on the results presented, the following conclusions can be made:

1. It should be noted that the true ratio of  $F_{3D}/F_{2D}$  has been bracketed by the numerical upper and lower bound analysis within a range of  $\pm 10\%$  or better for all cases considered. The ratio of  $F_{3D}/F_{2D}$  is found to increase with decreasing  $\beta$  and decreasing  $L/2H$ .

2. For the application example presented, the difference between the upper and lower bound factors of safety is found to be around 17% and for other quantities of  $L/2H$ , the safety factors for the 3D solutions are around 1 to 1.17 times that of the safety factors of the 2D solutions.

3. The stability number  $N_s$  decreases when  $\beta$  and the  $L/2H$  ratio increase. For a given  $\beta$ ,  $N_s$  achieves the minimum value when  $L/2H$  goes to infinite. This implies that the factor of safety will reduce with increasing  $L/2H$  ratio.

4. Changing the relative curvature radius of slope ( $R_0/H$ ) shows that convex slopes in plan view are more stable than straight slopes. In general, the smaller the ratio  $R_0/H_0$  is, the higher the stability of convex slope in plan view.

5. The effect of curvature on the stability of convex slopes is less for steeper slopes.

6. It should be mentioned that with decreasing  $\lambda_{\phi c}$ , three-dimensional effects are more significant. In other words, the effect of curvature of slope is more important in cohesive soils.

**Acknowledge:** The paper has been supported by International Institute of Earthquake Engineering and Seismology (IIEES) and prepared in the framework of researches in seismic design of slopes in continuation and development of the research project No. 245-6302. This support is acknowledged.

## References

- [1] Taylor, D.W.:1948, Fundamentals of soil mechanics. New York: John Wiley & Sons, Inc.
- [2] Bishop, A.W.:1955, The use of slip circle in stability analysis of slopes. *Geotechnique*; 5(1):7–17.
- [3] Morgenstern, N.:1963, Stability charts for earth slopes during rapid drawdown. *Geotechnique*; 13:121–31.
- [4] Griffiths, D.V, Lane, P.A.:1999, Slope stability analysis by finite elements. *Geotechnique*; 49(3):387–403.
- [5] Michalowski, R.L.:1989, Three-dimensional analysis of locally loaded slopes. *Geotechnique*; 39(1):27–38.
- [6] Xie M, Esaki T, Zhou G, Mitani Y.:2003, Geographic information systems-based three-dimensional critical slope stability analysis landslide hazard assessment. *J Geotech Geoenviron Eng ASCE*; 129(12):1109–18.
- [7] Janbu N, Bjerrum L, Kjaernsli B.:1956, Soil mechanics applied to some engineering problems. Norwegian Geotechnical Institute. Publication 16.
- [8] Gens A, Hutchinson J.N, Cavounidis S.:1988, Three-dimensional analysis of slides in cohesive soils. *Geotechnique*; 38(1):1–23.
- [9] Hovland H.J.: 1977, Three-dimensional slope stability analysis method. *J Geotech Eng Div ASCE*;103(9):971–86.
- [10] Hungr O.:1987, An extension of Bishop's simplified of slope stability analysis to three-dimensions. *Geotechnique*;37(1):113–7.
- [11] Leshchinsky D, Baker R.: 1986, Three-dimensional slope stability: end effects. *SoilsFound*;26(4):98–110.
- [12] Spencer E.: 1967, A method of analysis of the stability of embankments assuming inter-slice forces. *Geotechnique*;17(1):11–26.
- [13] Morgenstern NR, Price VE.:1965, The analysis of the stability of general slip surfaces. *Geotechnique*; 15(1):79–93.
- [14] Giger M. W., Krizek R. J.:1975, Stability analysis of vertical cut with variable corner angle. *Soils Found.*, 15(2): 63–71.
- [15] Giger M. W., Krizek R. J. :1976, Stability of vertical corner cut with concentrated surcharge load." *J. Geotech. Engrg. Div.*, 102(1): 31–40.
- [16] Baker R., Leshchinsky D. :1987, Stability analysis of conical heaps. *Soils Found.*, 27(4): 99–110.
- [17] Xing Z. :1988, Three-dimensional stability analysis of concave slopes in plan view. *J. Geotech. Engrg.*, 114(6): 658–671.
- [18] Ohlmacher G. C. :2007, Plan curvature and landslide probability in regions dominated by earth flows and earth slides." *Eng. Geol. (Amsterdam)*, 91: 117–134.
- [19] Leshchinsky, D., Baker, R., and Silver, M. L. :1985. "Three-dimensional analysis of slope stability." *Int. J. Numer. Analyt. Math. Geomech.*, 9: 199–223.
- [20] Michalowski R. L. :1989, Three dimensional analysis of locally loaded slopes. *Geotechnique*, 39(1): 27–38.
- [21] Farzaneh O, Askari F.:2003, Three-dimensional analysis of nonhomogeneous slopes. *JGeotech Geoenviron Eng ASCE*;134(8):137–45.
- [22] Duncan J.M.: 1996, State of the art: limit equilibrium and finite-element analysis of slopes. *J Geotech Eng ASCE*;129(2):577–96.
- [23] Farzaneh O, Askari F.: 2008, Three-dimensional stability analysis of convex slopes in plan view. *JGeotech Geoenviron Eng ASCE* 2008; 129(2):1090–0241.
- [24] Chen J, Yin JH, Lee CF.: 2003, Upper bound limit analysis of slope stability using rigid finite elements and nonlinear programming. *Can Geotech J*; 40:742–52.
- [25] Chen Z, Wang X, Haberfield C, Yin J-H, Wang Y.: 2001, A three-dimensional slope stability analysis method using the upper bound theorem part I. *Int J Rock Mech* 38:369–78.
- [26] Donald IB, Chen ZY. : 1997, Slope stability analysis by the upper bound approach:fundamentals and methods. *Can Geotech J*; 34:853–62.
- [27] De Buhan P, Garnier D.: 1998, Three dimensional bearing capacity analysis of a foundation near a slope. *Soils Found*; 38(3):153–63.
- [28] Michalowski RL.: 2002, Stability charts for uniform slopes. *J geotGeoenEnASCE*; 128(4):351–5.
- [29] Michalowski RL.: 1997, Stability of uniform reinforced slopes. *J Geotech Geoenviron Eng ASCE*;123(6):546–56.
- [30] Viratjandr C, Michalowski RL. : 2006, Limit analysis of submerged slopes subjected to water drawdown. *Can Geotech J*; 43:802–14.
- [31] Lyamin A.V, Sloan S.W.: 2002, Lower bound limit analysis using non-linear programming. *Int J Numer Methods Eng*;55:573–611.
- [32] Krabbenhoft K, Lyamin AV, Hjiaj M, Sloan SW.: 2005, A new discontinuous upper bound limit analysis formulation. *Int J Numer Methods Eng*; 63:1069–88.
- [33] Yu HS, Salgado R, Sloan SW, Kim JM.: 1998, Limit analysis versus limit equilibrium for slope stability. *J Geotech Geoenviron Eng ASCE*; 124(1):1–11.
- [34] Baligh, M. M., and Azzouz, A. S.:1975, End effects on stability of cohesive slopes. *J. Geotech. Engrg. Div.*, 101(11): 1105–1117.
- [35] Ugai K.: 1985, Three-dimensional stability analysis of vertical cohesive slopes. *SoilsFound*;25(3):41–8.
- [36] Farzaneh, O., and Askari, F.: 1994, 3D stability of slopes using upper bound limit analysis method, PhD thesis, Tehran University.

## Appendix 1: Linear Finite Element Formulations

As mentioned before, the finite element formulation is similar to those of Lyamin and Sloan [11], however in this study the types of meshes are differed and also these formulations are applied in seismic analysis.

The stresses, together with the body force components  $h_i$  which act on a unit volume of material, are taken as the problem variables. The vector of unknowns for an element  $e$  is denoted by  $x_e$  and may be written as

$$x^e = \{\{\sigma_{ij}^l\}^T, \dots, \{\sigma_{ij}^{D+1}\}^T, \{h_i\}^T\}^T, \quad (1)$$

$$i=1, \dots, D; j=i, \dots, D$$

where  $\{\sigma_{ij}^l\}$  are the stresses at node  $l$  and  $\{h_i\}$  are the elemental body forces. The variation of the stresses throughout each element may be written conveniently as

$$\sigma = \sum_1^4 N_l \sigma^l \quad (2)$$

where  $N_l$  are linear shape functions. The latter can be expressed as:

$$N_l = \frac{1}{|C|} \sum_0^3 (-1)^{l+k+1} |c_{(l)(k)}| x_k \quad (3)$$

where  $x_k$  are the coordinates of the point at which the shape functions are to be computed (with the convention that  $x_0=1$ ),  $C$  is a  $4 \times 4$  matrix formed from the element nodal coordinates according to

$$C = \begin{bmatrix} 1 & x_1^1 & x_2^1 & x_3^1 \\ 1 & x_1^2 & x_2^2 & x_3^2 \\ 1 & x_1^3 & x_2^3 & x_3^3 \\ 1 & x_1^4 & x_2^4 & x_3^4 \end{bmatrix} \quad (4)$$

and  $C_{(l)(k)}$  is a  $3 \times 3$  submatrix of  $C$  obtained by deleting the  $l$ th row and the  $k$ th column of  $C$ . In above expressions, the superscripts are row numbers and correspond to the local node number of the element, while the subscripts are the column numbers and designate the coordinate index. Elements in the first terms, Equation (2) can be written in the more compact form

$$N_l = \sum_0^3 a_{lk} x_k \quad (5)$$

$$a_{lk} = (-1)^{l+k+1} \frac{|c_{(l)(k)}|}{|C|} \quad (6)$$

### Element equilibrium

To generate a statically admissible stress field, the stresses throughout each element must obey the equilibrium equations

$$\frac{\partial \sigma_{ij}}{\partial x_j} + h_i = -g_i, \quad i = 1, 2, 3 \quad (7)$$

where  $\sigma_{ij}$  are Cartesian stress components, defined with respect to the axes  $x_j$ , and  $g_i$  and  $h_i$  are, respectively, prescribed and unknown body forces acting on a unit volume of material

within the element. Writing the governing equations in terms of stress vector, which reduces the number of unknowns, Equation (5) becomes in following matrix notation

$$A_{equil} x^e = b_{equil} \quad (8)$$

in which  $A_{equil}$  is coefficients matrix of equilibrium and  $b_{equil}$  is constant matrix of equilibrium. Thus, in total, the equilibrium condition generates 3 equality constraints on the element's variables in three dimensional modeling.

### Discontinuity equilibrium

To incorporate statically admissible discontinuities at interelement boundaries, it is necessary to enforce additional constraints on the nodal stresses. A statically admissible discontinuity requires continuity of the shear and normal components but permits jumps in the tangential stress. Since the stresses vary linearly along each element side, static admissibility is guaranteed if the normal and shear stresses are forced to be equal at each pair of adjacent nodes on an interelement boundary.

In the previous section, the components of the stress tensor  $\sigma_{ij}$  are defined with respect to the rectangular Cartesian system with axes  $x_j$ ,  $j=1,2,3$ . In addition to this global co-ordinate system, let us define a local system of Cartesian co-ordinates  $x'_k$ ,  $k = 1,2,3$ , with the same origin but oriented differently, and consider the stress components in this new reference system. Assuming these two coordinate systems are related by the linear transformation

$$x'_k = \beta_{kj} x_j, \quad k = 1, 2, 3 \quad (9)$$

where  $\beta_{ij}$  are the direction cosines of the  $x'_k$ -axes with respect to the  $x_j$ -axes, then the tractions acting on a surface element, whose normal is parallel to one of the axes  $x'_k$ , are given by the vector  $t^k$  with components

$$t_i^k = \sigma_{ij} \beta_{jk} \quad (10)$$

The corresponding transformation law for the stress components is

$$\sigma'_{km} = \sigma_{ij} \beta_{ki} \beta_{mj} \quad (11)$$

Using the definition of the stress vector, and assuming that the normal to the discontinuity plane is parallel to the axis  $x'_k$  (9) may be written as

$$A_{disc} x^e = b_{disc} \quad (12)$$

in which  $A_{disc}$  is coefficients matrix and  $b_{disc}$  is constant matrix. Hence the equilibrium condition for each discontinuity generates 9 equality constraints on the nodal stresses.

### Boundary conditions

Consider a distribution of prescribed surface tractions  $t_p$ ,  $p \in P$  where  $P$  is a set of  $N_p$  prescribed components, which act

over part of the boundary area  $A_l$ . For the case of a linear finite element, where the tractions are specified in terms of global coordinates over the linearized boundary area  $A_l^d$ , we can cast the stress boundary conditions for every node  $l$  as

$$\sigma_{ip}^l \beta_{ki}^l = t_p^l \quad (13)$$

Assuming the local coordinate system is chosen with  $x'_l$  parallel to the surface normal at node  $l$ , this type of stress boundary condition gives rise to the constraints

$$A_{bound} x^e = b_{bound} \quad (14)$$

in which  $A_{disc}$  is coefficients matrix and  $b_{disc}$  is constant matrix. Thus every node which is subject to prescribed surface tractions generates a maximum of 3 equality constraints on the unknown stresses.

### Assembly of Constraint Equations

All of the steps that are necessary to formulate the lower bound theorem as an optimization problem have now been covered. The only step remaining is to assemble the constraint matrices and objective function coefficients for the overall mesh. Using mentioned equations the various equality constraints may be assembled to give the overall equality constraint matrix according to

$$A_{global} = \sum_1^E A_{equil} + \sum_1^{D_s} A_{disc} + \sum_1^{B_n} A_{Bound} \quad (15)$$

where  $E$  is the total number of elements,  $D_s$  is the total number of discontinuities,  $B_n$  is the total number of boundary nodes which are subject to prescribed surface tractions. Similarly, the corresponding right-hand side vector  $b$  is assembled according to

$$b_{global} = \sum_1^E b_{equil} + \sum_1^{D_s} b_{disc} + \sum_1^{B_n} b_{Bound} \quad (16)$$

When the stress field is modeled using linear finite elements, the objective function and equality constraints are linear in the unknowns, with the only non-linearity arising from the yield inequalities. Thus the problem of finding a statically admissible stress field which maximizes the collapse load may be stated as

$$\begin{aligned} &\text{Maximize} && C^T x \\ &\text{Subject to} && Ax = b \\ & && f_j(x) \leq 0; j \in R^n \\ & && x \in R^n \end{aligned} \quad (17)$$

where  $c$  is a vector of objective function coefficients of length  $n$ ,  $A$  is an  $m \times n$  matrix of equality constraint coefficients,  $f_j(x)$  are yield functions and other convex inequality constraints and  $x$  is a vector of length  $n$  which is to be determined.